Temperature- and pressure-induced lattice distortion in $CdCr_{2-x}Ga_xSe_4$ (x = 0, 0.06, and 0.12)

2002 J. Phys.: Condens. Matter 14 12423

(http://iopscience.iop.org/0953-8984/14/47/315)

INSTITUTE OF PHYSICS PUBLISHING JOURNAL OF PHYSICS: CONDENSED MATTER

J. Phys.: Condens. Matter **14** (2002) 12423–12431 PII: S0953-8984(02)37777-4

Temperature- and pressure-induced lattice distortion in $CdCr_{2-x}Ga_xSe_4$ (x = 0, 0.06, and 0.12)

A Waśkowska[1], L Gerward[2], J Staun Olsen[3] and E Malicka[4]

[1] Institute of Low Temperature and Structure Research, Polish Academy of Sciences, 50 422 Wroclaw, Poland
[2] Department of Physics, Technical University of Denmark, 2800 Kongens Lyngby, Denmark
[3] Niels Bohr Institute, Oersted Laboratory, University of Copenhagen, 2100 Copenhagen, Denmark
[4] Institute of Chemistry, Silesian University in Katowice, 40 007 Katowice, Poland

Received 7 June 2002, in final form 2 October 2002
Published 15 November 2002
Online at stacks.iop.org/JPhysCM/14/12423

Abstract

Structural changes in the cubic spinels $CdCr_{2-x}Ga_xSe_4$ have been studied by means of single-crystal x-ray diffraction at low temperature and energy-dispersive diffraction in a diamond-anvil cell at high pressure. In stoichiometric samples ($x = 0$), a spontaneous magnetostriction reduces the thermal expansion coefficient from 6.7×10^{-6} K^{-1} in the paramagnetic phase to 2.2×10^{-6} K^{-1} in the ferromagnetic phase ($T_C = 130$ K). In the samples with Ga^{3+} admixtures ($x = 0.06$ and 0.12), a slight structural distortion causes an order–disorder-type phase transition at $T_d \approx 285$ K connected with changes in the electronic configuration of the Jahn–Teller-active Cr cations. The magnetostriction is apparently not very sensitive to the Ga^{3+} admixtures in the present concentration range. At high pressure the cubic unit cell transforms to a tetragonal one with $c/a = 0.91$. The Jahn–Teller effect is combined with the rocking motions of corner-sharing metal coordination polyhedra, altering their shape. The transition pressure is about 10 GPa. The bulk modulus of the cubic phase is $B_0 = 103$ GPa.

(Some figures in this article are in colour only in the electronic version)

1. Introduction

Pure $CdCr_2Se_4$ combines ferromagnetic and semiconducting properties. It crystallizes in the cubic spinel structure, space group $Fd\bar{3}m$, with lattice constant $a = 10.754$ Å. It has a normal cation distribution, the Cd^{2+} ions being located at the tetrahedral interstitial sites of the selenium sublattice, and the Cr^{3+} ions at the octahedral sites. The magnetic properties result from two main interactions: the coupling between the 3d electrons of the nearest-neighbour (nn) Cr^{3+} ions, and the weaker antiferromagnetic spin exchange between the next-nearest-neighbour (nnn) ions [1–6]. The range 129–142 K of the reported values for the Curie

temperature, T_C, indicates that the compound is sensitive to non-stoichiometry [7, 8]. Pure $CdCr_2Se_4$ is a p-type semiconductor. However, it can be changed to n-type by doping, e.g. with indium [9]. Also, the magnetic properties can be modified by chemical substitution.

Recently, Okońska-Kozłowska *et al* [10] have shown that small amounts of Ga^{3+} admixture, giving $CdCr_{2-x}Ga_xSe_4$ ($x = 0$–0.13), can alter the spin configuration from ferromagnetic to antiferromagnetic type. Substitution of non-magnetic gallium into the Cr^{3+} sublattice does not change the crystal structure at room temperature but causes a weakening of the Cr–Cr coupling, as was confirmed by a decreasing saturation magnetization with increasing Ga concentration. T_C is observed to shift from 130 to 120 K, as x varies from 0 to 0.06. The gallium concentration $x = 0.13$ greatly limits the magnitude of the ferromagnetic coupling, and the compound is antiferromagnetic below the Néel temperature, $T_N = 214$ K.

Strong magnetic interactions may produce spontaneous magnetostriction (magnetoelastically induced strains), which manifests itself as a contraction or expansion of the unit cell (see e.g. [11]). This effect has been reported for various types of magnetic material [12–15]. It has been suggested that the strength of the nn interaction decreased rapidly with increasing lattice constants. In contrast, the nnn interactions are less sensitive to changes in the unit-cell dimensions.

A first report on a low-temperature lattice dilatation in $CdCr_2Se_4$ was given by Martin *et al* [16], who observed some anomalies in the expected contraction of the unit cell with decreasing temperature. The volume change, which was of the order of 0.1%, was found to be small compared with thermodynamic predictions based on values of dT_C/dp and the magnetic energy, as determined from the high-temperature susceptibility [17].

The aim of the present work is to study the effect of temperature and hydrostatic pressure on possible crystal unit-cell distortions of $CdCr_{2-x}Ga_xSe_4$ ($x = 0$, 0.06, and 0.12) using x-ray diffraction. Since magnetic interactions depend on interatomic distances, we expect unit-cell anomalies at low temperatures and high pressures. Studies of this kind should make it possible to draw conclusions on the effect of Ga^{3+} admixtures on the exchange mechanisms and the stability of the cubic spinel structure.

2. Experimental details

2.1. Sample preparation

Single crystals of $CdCr_{2-x}Ga_xSe_4$ ($x = 0$–0.12) were grown by vapour transport in a closed quartz ampoule which contained CdSe and Ga_2Se_3 in a solid form. Anhydrous $CrCl_3$ was used as the chemical transport agent. Details of the syntheses have been given elsewhere [10, 18].

2.2. Low-temperature measurements

The unit-cell parameters of single crystals were measured with a Huber four-circle diffractometer using synchrotron radiation from the positron storage ring DORIS III at HASYLAB/DESY in Hamburg, Germany (Station D3). The energy of the orbiting positrons was 4.5 GeV, corresponding to a critical photon energy of $E_c = 16.6$ keV. A tunable double-crystal monochromator provided x-rays with wavelength $\lambda = 0.5596$ Å.

The samples were cooled down to a lowest temperature of about 95 K with an Oxford Cryostream attachment. For all samples, 26 high-angle reflections of the classes $\{8\,8\,8\}$ and $\{3\,3\,13\}$ ($2\theta \approx 42°$, where θ is the Bragg angle) were centred. Their angular positions were used in a least-squares refinement of the unit-cell parameters with no symmetry constraints being imposed. The estimated standard deviations (esd) were sample dependent and usually

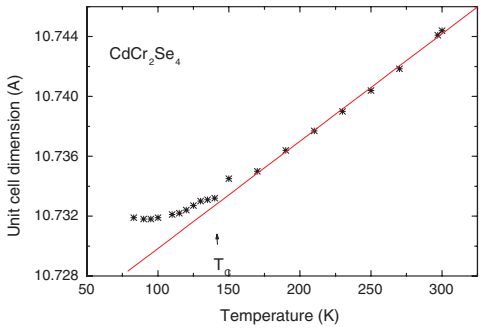

Figure 1. The lattice constant of $CdCr_2Se_4$ as a function of temperature upon cooling. The solid line is a linear extrapolation from the temperature region corresponding to the paramagnetic phase.

in the range from 0.0006 to 0.002 Å. However, at temperatures lower than 105 K, the esds increased to about 0.003 Å due to a poorer temperature stabilization. X-ray rotation photographs about selected crystal directions were made in order to control the crystal symmetry above and below T_C.

2.3. High-pressure measurements

High-pressure powder diffraction patterns were recorded at room temperature using the white-beam energy-dispersive method and synchrotron radiation (Station F3 of HASYLAB, Hamburg, Germany). High pressures up to 30 GPa were obtained in a Syassen–Holzapfel-type diamond-anvil cell. A finely ground powder sample and a ruby chip were placed in a 200 μm diameter hole of an Inconel gasket, preindented to a thickness of 60 μm. Silicone oil or a 16:3:1 methanol:ethanol:water mixture was used as the pressure-transmitting medium. The pressure was determined by measuring the wavelength shift of the ruby R_1 and R_2 luminescence lines and applying the non-linear pressure scale of Mao *et al* [19]. The Bragg angle was calculated from a zero-pressure diffraction spectrum of NaCl in the diamond-anvil cell. The standard deviation of the pressure determination was about 0.1 GPa for pressures up to about 10 GPa. For higher pressure the esd might be larger because of possible non-hydrostatic conditions.

Single-crystal, high-pressure unit-cell measurements at room temperature were also performed using a Kuma KM-4 diffractometer and a laboratory x-ray source (Mo Kα radiation, $\lambda = 0.71073$ Å).

2.4. Results

2.5. Low-temperature data

Unit-cell dimensions as functions of temperature for $CdCr_{2-x}Ga_xSe_4$ crystals with $x = 0$, 0.06, and 0.12 are given in figures 1 and 2. The stoichiometric sample contracts linearly in the paramagnetic phase upon cooling (figure 1). However, close to T_C we observe a deviation from the expected non-magnetic Grüneisen–Debye behaviour [20]. The thermal expansion coefficient $\alpha(T)$ can be written as follows:

$$\alpha(T) = \frac{\Gamma C_V(\theta_D/T)}{3B_0V_{mol}} \tag{1}$$

where $\alpha(T)$ is the thermal expansion coefficient, Γ is the Grüneisen constant, B_0 is the bulk modulus, T is the temperature, θ_D is the Debye temperature, V_{mol} is the molar volume, and

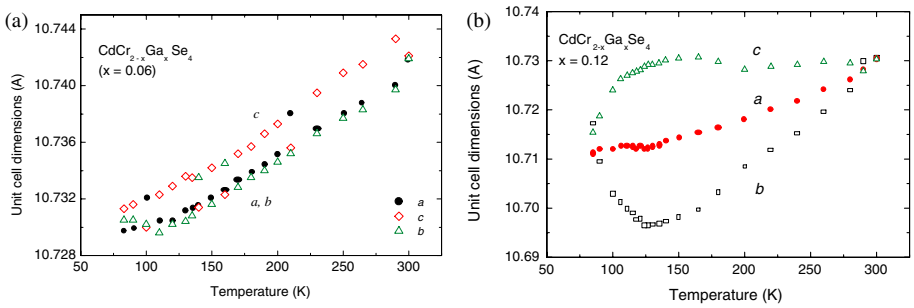

Figure 2. Unit-cell dimensions of single-crystal $CdCr_{2-x}Ga_xSe_4$ as functions of temperature upon cooling. (a) A sample with the Ga concentration $x = 0.06$. At 100, 140, 160, and 210 K the interchange of the axes (a, b) and c can be observed. (b) A sample with the Ga concentration $x = 0.12$.

C_V (θ_D/T) is the temperature-dependent specific heat. Since we could not determine the specific heat and the Debye temperature, we made a linear extrapolation of the temperature behaviour of the unit cell in the paramagnetic phase, as shown by the solid line in figure 1. The local anomaly close to T_C is caused by a spin ordering and magnetization increase in the ferromagnetic phase. Also, the magnetic interactions appear to be strong enough to be preserved in the short-range domains persisting in the paramagnetic state for $T > T_C$. The linear thermal expansion coefficient, defined by

$$\alpha = \frac{1}{a_0}\frac{\Delta a}{\Delta T}, \tag{2}$$

is 6.68×10^{-6} K^{-1} in the paramagnetic phase ($300 > T > 165$ K), and 2.18×10^{-6} K^{-1} in the ferromagnetic phase ($130 > T > 95$ K).

The temperature-dependent variation of the unit-cell dimensions has been studied for several samples with the Ga^{3+} content $x = 0.06$. An example is shown in figure 2(a). The rotation pictures at $T = 190$ K show reflections split about one of the pseudocubic axes, indicating a tetragonal distortion (figure 3). The separation of the reflections is too small, however, to allow an adequate indexing of the reflections. The tetragonal deformation begins at $T_d \approx 290$ K and persists down to the lowest temperature of the present work (about 95 K). The c/a ratio is sample dependent, ranging from 1.000 18 to 1.000 29. The observed variation is probably due to minute differences in sample composition. Small anomalies in the temperature dependence of the unit-cell dimensions accompany the ferromagnetic-to-paramagnetic phase transition. Figure 2(a) also indicates an interchange of the a-and c-axis, suggesting a coexistence of cubic and tetragonal domains.

In the antiferromagnetic compound ($x = 0.12$), the main feature is an orthorhombic distortion (figure 2(b)). Like for the crystal with $x = 0.06$, the onset of the distortion occurs at $T_{d1} \approx 285$ K. The cubic-to-orthorhombic distortion is seen to increase with decreasing temperature, reaching a maximum close to T_C. The orthorhombic phase is not stable down to the lowest observed temperature: at $T_{d2} \approx 90$ K the crystal retains the symmetry valid for $T > T_{d1}$. Such behaviour has been described in terms of highly degenerate crystal-field levels [21] but this effect is beyond the scope of the present paper.

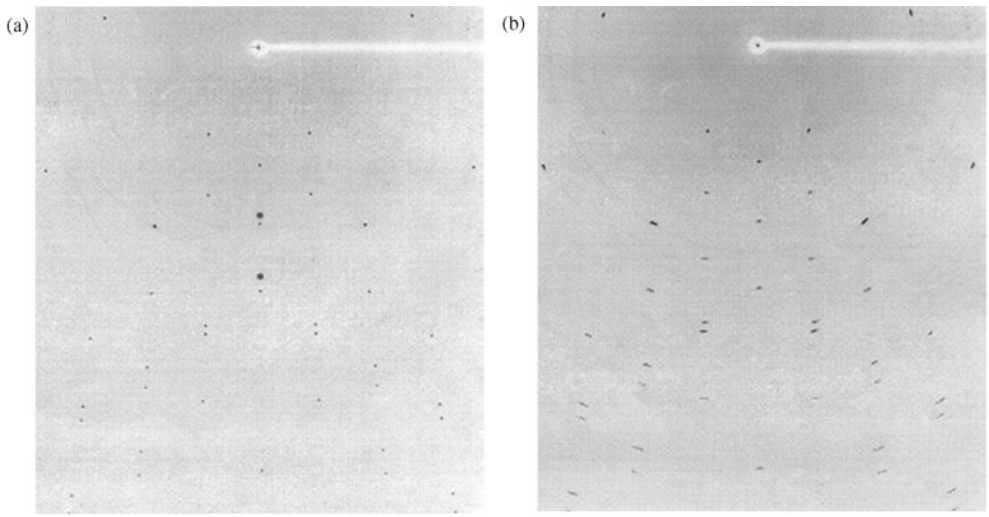

Figure 3. Rotation photographs, about the [011] direction of the pseudocubic cell of $CdCr_{2-x}Ga_xSe_4$ ($x = 0.06$). (a) Room temperature; (b) $T = 190$ K.

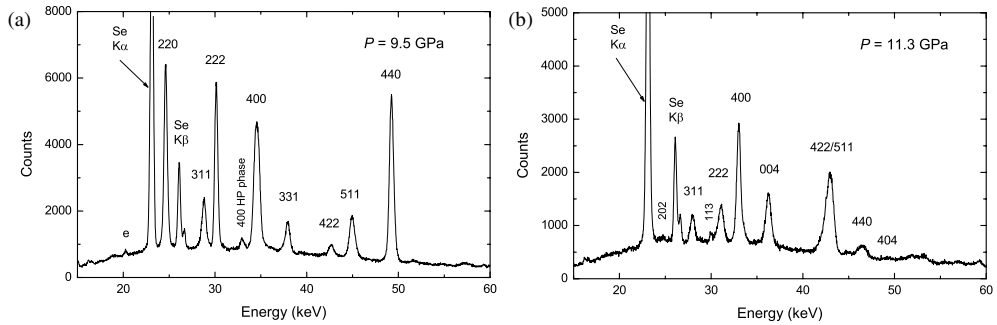

Figure 4. Indexed energy-dispersive diffraction patterns of $CdCr_2Se_4$. The Bragg angle $\theta = 3.922°$. (a) The cubic phase at 9.5 GPa. A weak 400 peak of the high-pressure phase is seen at 32.9 keV as a precursor of the cubic-to-tetragonal transition. (b) The tetragonal phase at 11.3 GPa. Notice the doublets 311/113, 400/004, and 440/404, whereas the 222 peak represents a single line.

2.6. High-pressure data

The high-pressure x-ray powder diffraction indicates that there is a structural pressure-induced phase transformation at about 10 GPa. Figure 4(a) shows an energy-dispersive diffraction pattern at 9.5 GPa. All lines, except one, can be indexed according to the cubic low-pressure phase. A weak 400 peak of the high-pressure phase is seen at 32.9 keV as a precursor of the transition. In comparison, figure 4(b) shows the diffraction pattern at 11.3 GPa where the sample is completely transformed to the high-pressure phase. The corresponding diffraction data are given in table 1. The goodness of the fit can be described by a goodness factor, G, given by

$$G = \sum |d_{obs} - d_{calc}| \Big/ \sum d_{obs} \tag{3}$$

Table 1. Diffraction data for the tetragonal high-pressure phase of $CdCr_2Se_4$ at 11.3 GPa (cf figure 4(b)). The refined lattice constants are $a = 10.90(6)$ Å and $c = 9.86(9)$ Å, where the uncertainties are the standard errors of the least-squares fit.

hkl	d_{obs} (Å)	d_{calc} (Å)
202	3.655	3.656
311	3.240	3.254
113	3.024	3.023
222	3.013	3.037
400	2.730	2.726
004	2.484	2.465
422		2.185
	2.112	
511		2.089
440	1.936	1.927
404	1.831	1.828

where d_{obs} and d_{calc} are the observed and calculated lattice-plane spacings. The 422 and 511 peaks are not resolved. Since the intensity of the 511 reflection is about twice that of the 422 reflection, the observed d-spacing should be compared with a weighted mean value $\langle d_{calc} \rangle = 2.121$ Å. We get $G = 0.4\%$, which is reasonably good for a high-pressure, energy-dispersive diffraction spectrum.

The diffraction patterns of the high-pressure phase can be indexed according to a tetragonal distortion of the fcc unit cell of the low-pressure phase; cf [22]. The 400/004 doublet, which shows up very clearly in figure 4(b), can be readily identified. In the tetragonal system, the 400 line is about twice as strong as the 004 line because of the multiplicity factor. It is seen that the 400 peak occurs at a lower energy than the 004 peak, indicating that the d-spacing of the (400) planes is larger than that of the (004) planes. Thus, it is concluded that the c/a ratio of the distorted fcc unit cell is less than one.

Figure 5 shows the lattice constants for the cubic and tetragonal phases as functions of pressure. Also shown in the figure is the c/a ratio, which, by definition, is unity for the cubic phase, and is found to be 0.91 for the tetragonal phase, independent of pressure. Given the experimental uncertainty, it has not been possible to detect any volume difference between the two phases at the transition pressure. The compression of the cubic phase can be described by the Birch equation of state [23]:

$$P/B_0 = \tfrac{3}{2}(\xi^{-7} - \xi^{-5})[1 + \tfrac{3}{4}(B_0' - 4)(\xi^{-2} - 1)] \tag{4}$$

where: $\xi = a/a_0$, a being the lattice constant at pressure P and a_0 the zero-pressure lattice constant. B_0 is the bulk modulus and B_0' its pressure derivative, both parameters evaluated at zero pressure. In the present work, we have fitted equation (3) to most of the experimental data, assuming $B_0' = 4.0$, which is a typical value for most solids. Table 2 shows compressibility data obtained by single-crystal diffraction and monochromatic x-rays (Mo Kα). We have also made several runs, using powder diffraction and the white-beam energy-dispersive method. As a final result, we quote $B_0 = 103(1)$ GPa and $B_0' = 4.0$. To the best of our knowledge, there are no literature data with which to compare the present result.

3. Discussion and conclusions

Regarding the temperature-dependent behaviour of the lattice parameters of the system $CdCr_{2-x}Ga_xSe_4$, two different phenomena should be considered. First, the magnetostriction,

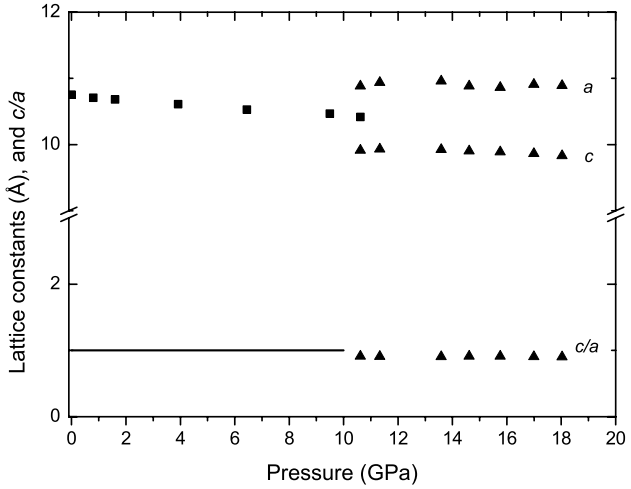

Figure 5. Lattice constants for the cubic and tetragonal phases as functions of pressure. Also shown is the c/a ratio.

Table 2. Compressibility data for cubic $CdCr_2Se_4$ obtained by means of high-pressure single-crystal diffraction. V is the unit-cell volume at pressure P, and V_0 is the zero-pressure volume. A fit of the Birch equation (3) to these data gives $B_0 = 104 \pm 4$ GPa and $B_0' = 3.3 \pm 1.9$, or $B_0 = 103.3 \pm 0.8$ GPa and $B_0' = 4.0$ (fixed), where the uncertainties are the standard errors of the least-squares fit.

P (GPa)	V/V_0
0.00	1.0000
0.65	0.9935
0.80	0.9929
1.22	0.9888
1.40	0.9874
1.65	0.9846
1.95	0.9816
2.15	0.9795
2.45	0.9769
2.75	0.9747
2.85	0.9734
3.40	0.9704
4.05	0.9647
4.60	0.9598

leading to the local anomalous volume increase, is connected with spin ordering between the Cr ions in the cubic cell. This effect has been observed in the stoichiometric sample (figure 1).

Second, a small structural distortion may be related to the changes in the electronic structure of the Cr^{3+} ions. The gallium admixtures or some deficit of selenium may cause a superexchange of the type Cr^{3+}–Se–$Cr^{3+} \rightarrow Cr^{2+}$–Se–$Cr^{4+}$, thereby producing strongly Jahn–Teller-active Cr^{2+} ions. According to the Jahn–Teller theorem, it is possible to lower the energy of the ground state by local deformation of the octahedral sites. The effect gives rise to a localized strain, when the lattice adjusts itself to the different radii of the three ions ($r_{Cr}^{2+} = 0.73$; $r_{Cr}^{3+} = 0.615$; $r_{Ga}^{3+} = 0.620$ Å). This mechanism seems to be the dominating one

for the chemically substituted samples, where small changes in crystal symmetry are observed at T_d.

Perturbations in the periodicity of the chromium octahedral sublattice destroy some paths of the long-range spin exchange between the Cr^{3+} electrons, inducing perturbations also in the ferromagnetic interactions. Although the symmetry is still very close to cubic at room temperature, the free energy does not have a stable minimum. In the samples with $x = 0.06$ and 0.12, small tetragonal and orthorhombic distortions of the lattice take place at $T_d \approx 285$ K in the paramagnetic phase. The actual temperature is sample dependent, varying from 280 to 290 K, since it is probably associated with a coexistence of cubic and tetragonal domains. The structural differences may be a result of fluctuations in the positional parameter, u, of the selenium ions. The distortions are small, however, for the gallium concentrations used in this work. Therefore, the splitting of the Bragg reflections is not sufficient to allow for a complete space-group determination.

In conclusion, the magnetoelastic properties are apparently not very sensitive to the presence of the Ga^{3+} admixtures. However, since the magnitude of magnetostriction depends mainly on the Cr–Cr interactions, it is slightly weaker in the samples with Ga^{3+} dopants. The structural deformations in the samples with $x = 0.06$ and 0.12 are associated with the chemical substitution and the resulting change in the electronic structure of the magnetic Cr^{3+} ion.

At high pressure, the enhanced Jahn–Teller effect should be combined with rocking movements of corner-sharing metal coordination polyhedra. These movements require some changes in Se–Se distances; therefore the polyhedra are not rigid any longer and alter their shape. The axial ratio $c/a < 1$, which means that the polyhedra become contracted (flattened). At high pressure the macroscopic deformation is more pronounced compared to the temperature-dependent effects. This makes it possible to determine the crystal symmetry as tetragonal.

It has been observed that normal spinel oxides with the chemical formula AB_2O_4 have about the same response to hydrostatic pressure. The zero-pressure bulk moduli of these compounds have been found to be around 200 GPa (e.g. [24–26]). This behaviour, which was obtained empirically by Finger *et al* [27], has recently been confirmed theoretically by Pendás *et al* [28]. Essentially, the explanation is that the oxygen anions are forming a nearly close-packed fcc substructure, occupying most of the available volume. In this way, the overall compressibility is determined mainly by the oxygen ions.

In accordance with the arguments given above, it may be assumed that the compressibility of the selenium-based spinels is determined mainly by the selenium substructure. The experimental result of the present work indicates that the selenium cubic spinels, having a bulk modulus of about 100 GPa, show higher compressibility than the oxides. The lower ionicity and the greater metallic character of the chemical bonding in $CdCr_2Se_4$ as compared with the oxygen spinels can explain the observed difference in compressibility. Theoretical work to clarify this point is in progress.

Acknowledgments

The authors thank HASYLAB-DESY, Germany, for permission to use the synchrotron facility and the Danish Natural Sciences Research Council (DANSYNC) for financial support. The work was sponsored by the IHP Programme *Access to research infrastructures* of the European Community under contract No HPRI-CT-1999-00040.

References

[1] Baltzer P K, Lehmann W H and Robbins M 1965 *Phys. Rev. Lett.* **15** 493
[2] Baltzer P K, Wojtowicz P J, Robbins M and Lopatin E 1966 *Phys. Rev.* **151** 367
[3] Lehmann W H and Robbins M 1966 *J. Appl. Phys.* **37** 1389
[4] Goodenough J B 1967 *J. Phys. Chem. Solids* **30** 261
[5] Haas C, van Run A M J G, Bongers P F and Albers W 1967 *Solid State Commun.* **5** 657
[6] Menyuk N, Dwight K, Arnott R J and Wold A 1966 *J. Appl. Phys.* **37** 1387
[7] LeCraw R C, von Philipsborn H and Sturge D 1967 *J. Appl. Phys.* **38** 946
[8] Bel'skii N K, Ochertyanova L I, Shabunina G G and Aminov T G 1985 *Neorg. Mater.* **21** 496
[9] Lehmann W H 1967 *Phys. Rev.* **163** 488
[10] Okońska-Kozłowska I, Malicka E, Waśkowska A, Heimann J and Mydlarz T 2001 *J. Solid State Chem.* **158** 34
[11] Shiga M and Nakamura Y 1969 *J. Phys. Soc. Japan* **26** 24
[12] Andreyev A, Javorsky P and Lindbaum A 1999 *J. Alloys Compounds* **290** 10
[13] Kusz J, Boehm H and Talik E 2000 *J. Appl. Crystallogr.* **33** 213
[14] Brabers J H V J, Buschow K H J and De Boer F R 1999 *Phys. Rev.* B **59** 9314
[15] Ono H, Shimada H and Toma H 2000 *J. Appl. Phys.* **88** 7213
[16] Martin G W, Kellog A T, White R I and White R M 1969 *J. Appl. Phys.* **40** 1015
[17] Bindloss W 1971 *J. Appl. Phys.* **42** 1474
[18] Malicka E 2000 *PhD Thesis* Institute of Chemistry, Silesian University in Katowice, Poland
[19] Mao H K, Xu J and Bell P M 1986 *J. Geophys. Res.* B **91** 4673
[20] Krishnan R S, Srinivasan R and Devanarayanan S 1979 Thermal expansion of crystals *(Int. Ser. in Science of the Solid State vol 12)* ed R Pamplin (Oxford: Pergamon)
[21] Sevardière J 1972 *Phys. Rev.* B **6** 4284
Sevardière J 1973 *Phys. Rev.* B **8** 2004
[22] Gerward L, Staun Olsen J and Benedict U 1986 *Physica* B **144** 72
[23] Birch F 1938 *J. Appl. Phys.* **9** 279
[24] Åsbrink S, Waśkowska A, Staun Olsen J and Gerward L 1998 *Phys. Rev.* B **57** 4972
[25] Åsbrink S, Waśkowska A, Gerward L, Staun Olsen J and Talik E 1999 *Phys. Rev.* B **60** 12651
[26] Waśkowska A, Gerward L, Staun Olsen J, Steenstrup S and Talik E 2001 *J. Phys.: Condens. Matter* **13** 2549
[27] Finger L W, Hazen P M and Hofmeister A 1986 *Phys. Chem. Minerals* **13** 215
[28] Pendás A M, Costales A, Blanco M A, Recio J M and Luaña V 2000 *Phys. Rev.* B **62** 13970